BG

PREPRINT

TASCC-P-96-7

tascc

Evolution of Fragment Production as a Function of Excitation in ^{35}Cl and ^{70}Ge Projectile Breakup

L. Beaulieu[1], D.R. Bowman[2], D. Fox[2*], S. Das Gupta[4], J. Pan[4], G.C. Ball[2], B. Djerroud[1†], D. Doré[1‡], A. Galindo-Uribarri[2], D. Guinet[3], E. Hagberg[2], D. Horn[2], R. Laforest[1§], Y. Larochelle[1], P. Lautesse[3], M. Samri[1], R. Roy[1], and C. St-Pierre[1]

1 *Laboratoire de Physique Nucléaire, Département de Physique, Université Laval, Sainte-Foy, Québec, Canada G1K 7P4*

2 *AECL, Chalk River Laboratories, Chalk River, Ontario, Canada K0J 1J0*

3 *Institut de Physique Nucléaire de Lyon, 46 Bd du 11 Novembre 1918, F-69622, Villeurbanne Cedex, France*

4 *Department of Physics, McGill University, 3600 University St., Montréal, Québec, Canada H3A 2T8*

* **Present address: Practical Political Consulting, East Lansing, MI 48823, USA**

† **Present address: NSRL, University of Rochester, N.Y., USA**

‡ **Present address: IPN Orsay, BP 91406 Orsay Cedex, France**

§ **Present address: AECL, Chalk River Laboratories, Chalk River, Ontario, Canada, K0J 1P0**

To be published in the Proceedings of the 12th Winter Workshop on Nuclear Dynamics Snowbird, Utah, 3-10 Feb 1996

Physical and Environmental Sciences
Chalk River Laboratories
Chalk River, ON K0J 1J0 Canada

1996 April

Evolution of Fragment Production as a Function of Excitation in ^{35}Cl and ^{70}Ge Projectile Breakup

L. Beaulieu,[1] D.R. Bowman,[2] D. Fox,[2*] S. Das Gupta,[4] J. Pan,[4] G.C. Ball,[2] B. Djerroud,[1†], D. Doré,[1‡], A. Galindo-Uribarri,[2] D. Guinet,[3] E. Hagberg,[2] D. Horn,[2] R. Laforest,[1§], Y. Larochelle,[1] P. Lautesse,[3] M. Samri,[1] R. Roy,[1] and C. St-Pierre,[1]

[1]Laboratoire de Physique Nucléaire, Département de Physique, Université Laval, Sainte-Foy, Québec, Canada G1K 7P4.
[2]AECL, Chalk River Laboratories, Chalk River, Ontario, Canada K0J 1J0.
[3]Institut de Physique Nucléaire de Lyon, 46 Bd du 11 Novembre 1918, F-69622, Villeurbanne Cedex, France.
[4]Department of Physics, McGill University, 3600 University St., Montréal, Québec, Canada H3A 2T8.

INTRODUCTION

Intermediate-mass fragment (IMF) production, typically $3 \leq Z \leq 20$, is a widely observed decay mode in heavy-ion reactions[1]. Possible scenarios to explain such a decay mode include bulk instabilities based on the expansion of hot nuclear matter with an initial compression stage in near-central collisions [2]-[4]. However, for such collisions, dynamical IMF production is also present as is evident from the observation of neck emission[5]-[7]. Also, the persistence of binary dissipative collisions[8]-[11] leaves a very small cross section for forming a hot and dense single source[12, 13].

An alternate way to study highly excited nuclear matter is to consider the fast-moving source formed in peripheral collisions[14]-[31]. The Aladin collaboration, working at GSI, has explored the excitation energy dependence of IMF production from the breakup of the spectators in the reaction of Xe, Au and U projectiles on a gold target at 600 MeV/nucleon[32]. When scaled by the charge of the projectile, the average IMF number from all three projectiles was the same for a given excitation energy, suggesting that the IMF production mechanism is independent of the emitter size. This result

*Present address: Practical Political Consulting, East Lansing MI 48823, USA.
†Present address: NSRL, University of Rochester, N. Y., USA.
‡Present address: IPN Orsay, BP 91406 Orsay Cedex, France.
§Present address: AECL, Chalk River Laboratories, Chalk River, Ontario, Canada, K0J 1P0

is also consistent with the target independence already found in the Au-projectile-induced reactions at beam energies[33] of 400A, 600A and 1000A MeV, showing that the beam energy dependence could be removed by using the excitation energy. A global picture of the IMF production can be expressed by only two parameters, the excitation energy and the source size. In the case of a lighter system, namely ^{40}Ca at 35 MeV/nucleon[22, 23], the IMF emission was well reproduced by the sequential decay of a hot, rotating source[34] at variance with the Aladin data[35]. In the light system, the driving parameters for IMF production were the excitation energy and the angular momentum. Therefore, there seems to be a strong mass effect in the production mechanism.

In this paper, we explore IMF production as a function of the excitation energy for two systems, one in the range of the calcium study and the other between the first system and the Aladin Au experiments. Simulations with a standard sequential decay calculation for a hot, rotating source and with a lattice-gas model will be presented. The applicability of our results will be extended to a heavier system mass and higher beam energy by comparison to the Aladin work[32].

EXPERIMENTAL SET-UP and EVENT SELECTION

Experimental set-up

A ^{35}Cl beam at 43 MeV/nucleon and a ^{70}Ge beam at 35 MeV/nucleon from the TASCC facility at Chalk River bombarded self-supporting 2.9 mg/cm^2 ^{197}Au and 2.1 mg/cm^2 ^{nat}Ti targets. Charged particles were detected in the CRL-Laval forward array[36, 37] complemented with three telescopes at small angle. The array consists of 80 detectors mounted in 5 concentric rings around the beam axis and covering from 6.8° to 46.8°. The three inner rings are made of fast-slow plastic detectors with charge resolution up to Z=17 for the chlorine experiment and Z=20 for the germanium expriment. Energy thresholds are 7.5, 12.5 and 16.2 MeV/nucleon for Z=1,6 and 10 respectively. The two outer rings (24° to 46.8°) are made of CsI(Tl) crystals which achieve mass resolution for Z=1,2 and charge identification for Z=3. Ions with Z$\geq$4 were all attributed to Z=4. Thresholds are about 2.5 MeV/nucleon for Z=1,2 particles. Three Si-CsI(Tl) telescopes covered 18% of the solid angle between 3° and 5°, with charge resolution from Z=2 to 17 for the chlorine experiment and Z=2 to 32 for the germanium experiment. Typical thresholds were 2.5, 4.7 and 5.9 MeV/nucleon for Z=2,6 and 10 ions, respectively.

Event selection

The fast-moving emitter in the ^{35}Cl+Au reactions was selected according to the iterative procedure of Désesquelles *et al.*[23] and Lleres *et al.*[22]. In a first step, all particles with Z$\geq$4 detected in the phoswiches (high thresholds) were used to give a first estimate of the source velocity, about 84% of the beam velocity. At this stage, the particle-emission pattern in the reconstructed frame can be clearly seen. A selection is made in velocity space by accepting all charged particles moving in the forward direction. Particles emitted in the backward direction are attributed to the fast-moving source if their velocities are smaller than 4 cm/ns[22]. The data sample of events with a total charge of 17 consists of 580000 events. In the case of the ^{70}Ge+Ti reaction,

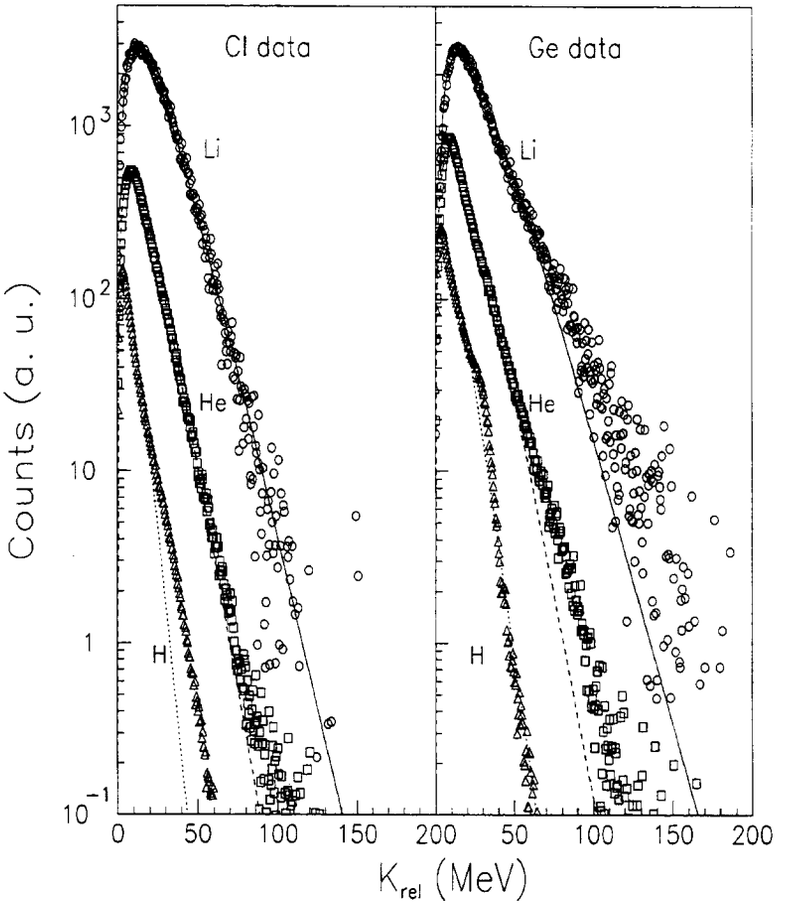

Figure 1. Kinetic energy spectra of Z=1,2 and 3 particles in the emitter frame. The Cl data are shown in the left part and the Ge in the right. The lines are Maxwell-Boltzman fits.

separation of the fast-moving source was more difficult and each particle having a laboratory velocity parallel to the beam and greater than or equal to 68% of the beam velocity was attributed to the fast emitter. More than 480000 events with a total charge from 29 to 33 were selected.

From these selected events, the emitter frame can be recontructed event by event. Fig. 1 shows the kinetic energy, in the emitter frame, for Z=1,2 and 3 particles from Cl (left) and Ge (right) projectiles. The distributions have been scaled so that Z=3 is displayed at the top. The lines through the data represent Maxwell-Boltzman fits and are shown only to demonstrate the shape of the emission. The Cl data are very well described by the fits with a small excess yield at high kinetic energy for Z=1. In the case of Ge data, there is an excess in both Li and He spectra but only at the 1% level. The shoulder in the Z=1 distribution is explained by the different acceptance of the CsI detectors. The overall emission pattern is in good agreement with that expected from a single isotropic source.

EXCITATION ENERGY

The first step in the evaluation of the excitation energy is to assign a mass to each charge and estimate the number of neutrons (which are undetected). This was done by taking the most abundant mass for each charge to perform a mass balance. Then, the excitation energy, E_1^*, is obtained by summing all the charged particles' kinetic energies in the emitter frame; a Q value, corrected for the neutrons, is added. Finally, the contribution of the kinetic energy of each neutron is taken to be $2 \times T$ or $2 \times \sqrt{8E_1^*/A}$.

The excitation energy distributions are shown in Fig. 2. In both cases, the distributions extend to high energies. The structure at low excitation is due to exit channels with charged particle multiplicities of 2, 3 and 4. The validity of high-excitation events was tested with the statistical code GENEVE[38]. This code first calculates the entrance channel and allows for pre-equilibrium emission of neutrons and protons. In a second step it proceeds with a deexcitation stage as in GEMINI[39]. Pre-equilibrium emission can lead to uncertainties of the order of 7% at energies above 10A MeV for the Cl data. Also, the tail of the distribution at 400 MeV and higher contains a 4% contribution from the target-like source. In the case of the Ge data, target emission is negligible because of the selection procedure used; uncertainties due to pre-equilibrium nucleons are estimated at a maximum of 10% for an excitation energy higher than 8.5A MeV. On the other hand, the GENEVE simulation did not consider a possible net mass transfer from the target to the projectile, which favors higher excitation[40].

FRAGMENT PRODUCTION

IMF number

The IMF distributions have been sorted as a function of excitation energy, which was divided into bins of 1A MeV width. The average number of IMF in each bin for Cl and Ge is shown in Fig. 3 as a function of the average excitation energy in each bin. The definition of an IMF is $3 \leq Z_{IMF} \leq 8$ for Cl and $3 \leq Z_{IMF} \leq 12$ for Ge. The

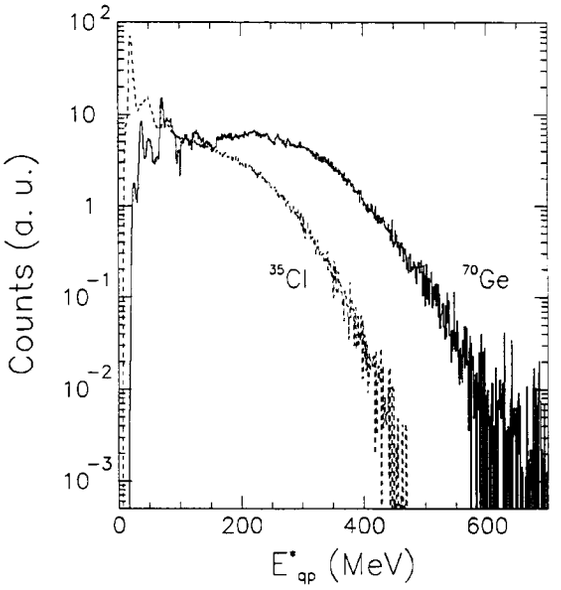

Figure 2. Excitation energy distributions for the Cl and Ge data.

maximum IMF production is reached at about 7A MeV of excitation in the Cl data and then decreases while the "fall of multifragmentation" is not reached in the Ge data.

A comparison to models was made first with a minimum number of parameters. This was achieved with the statistical code EUGENE[41]. Like GENEVE, EUGENE performs the calculation of the entrance channel, but without pre-equilibrium emission, shares the excitation energy and the angular momentum between the reaction partners, and simulates the sequential breakup of the excited target and projectile nuclei. The only adjustable parameters are the projectile and target masses and the beam energy. Each event is then filtered for detector acceptance and thresholds and treated exactly like the experimental data. The result of the simulations is shown for Cl in the upper part of Fig. 3. This model underpredicts the IMF production.

The second model used is the lattice-gas model[42, 43]. In this case, fragments are formed assuming a temperature and a freeze-out density. Based on the study of Ar+Sc by the MSU 4π group[42]-[44], the freeze-out density was chosen to be as close as possible to 0.39. This density ratio is given by the number of nucleons divided by the lattice size and is 0.35 for Cl (lattice size $4\times5\times5$) and 0.39 for Ge (lattice size $5\times6\times6$). Calculations are then made for increasing temperature values and filtered by a sotfware replica of the array. The simulations are displayed in Fig. 3 and show an overall agreement with the data.

The last model used was GEMINI. As in the calcium study by Lleres and co-workers[22], a correlation between excitation energy and angular momentum was used to reproduce the IMF number at each excitation energy. The angular momentum values used ranged from $0\hbar$ to $25\hbar$ for Cl and $0\hbar$ to $50\hbar$ for Ge, with the maximum values representing the critical angular momentum. The sequential breakup from a hot, rotating source is able to reproduce the IMF production over nearly all of the excitation energy range for the Cl data, quite similar to the calcium data[23]-[34]. The agreement is less successful above 7A MeV of excitation, which corresponds to the maximum of the angular momentum (kept constant at $25\hbar$); the model is pushed to the extreme in terms of excitation and angular momentum. For the Ge reaction, the agreement between GEMINI and the data is good for excitation up to 5A MeV but the IMF production saturates as the excitation energy increases to 8.5A MeV. The difference between the simulations and the data is greater than for the Cl data. Again, the importance of angular momentum in such models is evident in the simulations with $l=0\hbar$, where the IMF numbers are strongly underpredicted by the simulations.

Clearly, in GEMINI, the IMF production is dominated by angular momentum effects and is also strongly mass dependent. The maximum IMF number predicted by the code is higher in the Ge case by about 20% but the increase in the data is approximately 60%. The low excitation energy region is well reproduced in both cases. However, the lattice-gas model, which incorporates ingredients of prompt multifragmentation and phase instability, does better at high excitation and does not seem to suffer any mass dependence as in the GEMINI simulations. The connection between the two models, low and high excitation, suggests a change in the decay mechanism for IMF production and the importance of temperature in the lattice-gas model.

Mass scaling

Based on the Aladin results demonstrating beam-energy independence and mass scaling, we have compared the Cl and Ge IMF productions to the Aladin Au+Au data

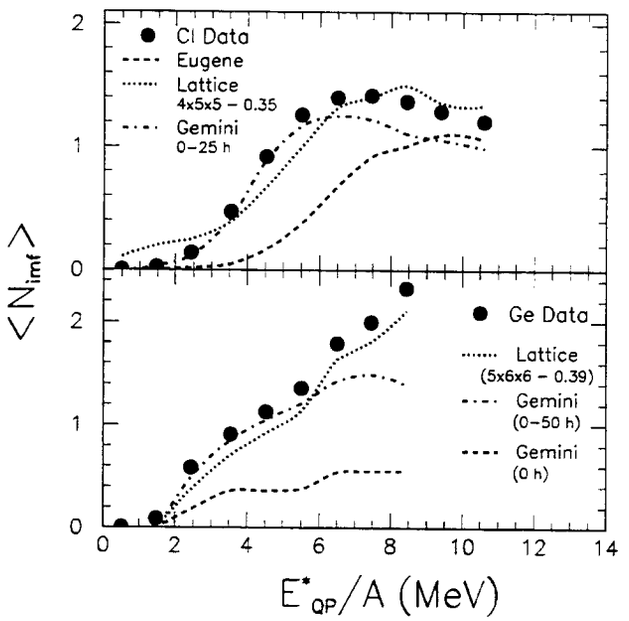

Figure 3. Average IMF number versus excitation energy per nucleon. Upper panel: Results of the Cl data are compared to simulations with EUGENE(dashed line), lattice-gas model(dotted line) and GEMINI(dash-dotted line). Bottom panel: Ge data and simulations with lattice-gas(dotted line) and GEMINI with (dash-dotted line) and without angular momentum(dashed line)

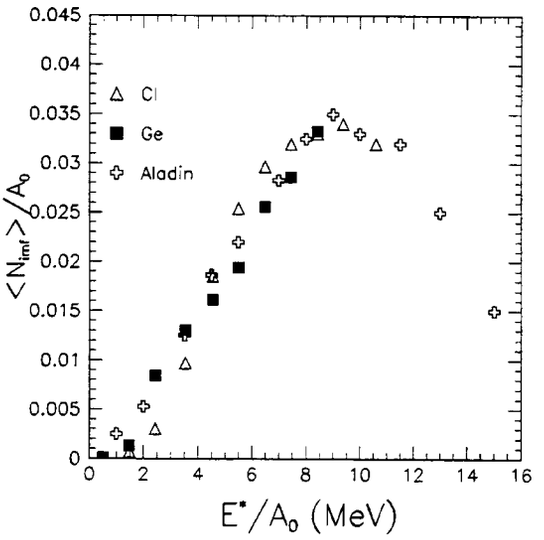

Figure 4. Scaled IMF numbers as a function of excitation per nucleon. The Cl and Ge data are shown and compared to the Aladin Au results from ref. 32.

at 600A MeV[47]. The excitation energy per nucleon, average IMF number and source size were extracted from ref. 32. The definition of an IMF was adjusted relative to the Aladin data by scaling the upper limits, $3 \leq Z_{IMF} \leq 30 \times (Z_{source}/79)$, Z=30 being the upper limit in the Aladin data. The new definition of an IMF is $3 \leq Z_{IMF} \leq 6$ for Cl and $3 \leq Z_{IMF} \leq 12$ for Ge data. Only the definition for the Cl reaction has changed in the process. Also, to fully compare the systems, the average IMF number was scaled at each excitation energy bin by the source size which is about constant for Cl and Ge because of the total charge requirement but decreases with increasing excitation for the Au data. The mass scaling results are shown in Fig. 4. The surprising result is that all curves coincide. There is also a strong correlation between the scaled number of IMF versus the excitation energy per nucleon, suggesting a temperature dependence for IMF production. As discussed previously, the overall curve would not be reproduced by GEMINI, the maximum IMF number being strongly mass dependent and decreasing as the mass increases. The data of Fig. 4 show that the IMF production relative to the system size is the same, in agreement with the lattice-gas model. It was also verified that the unfiltered lattice-gas simulations give the same mass scaling[47].

SUMMARY

IMF production has been studied as a function of excitation energy for two different systems, formed in Cl- and Ge-induced reactions. The average IMF numbers for the Cl reactions are well reproduced within the framework of a sequential decay of a hot rotating source with only a small discrepancy at high excitation. In contrast, only the low-excitation data are well reproduced for the Ge data. The comparison of the data to GEMINI calculations suggests a size effect in the IMF production mechanism as observed by Désesquelles *et al.*[48]. On the other hand, the lattice-gas model might be unrealistic at low excitation where GEMINI does well. However, the size effect is not present in the lattice-gas model which is in good agreement with both sets of data over the complete excitation energy range. By scaling the average IMF number by the source size, we were able to demonstrate a universal behaviour over a wide range of beam energies, from 35A MeV to 600A MeV, for a range of source masses, A$\sim$35-190. The thermal nature of IMF emission is evident in the strong correlation between the scaled IMF number and the excitation energy per nucleon, in good agreement with recent results by the EOS TPC collaboration[49, 50].

Acknowledgments

The authors would like to thank Dr. R.J. Charity (GEMINI), Dr. D. Durand (EUGENE) and Dr. J.P. Wielezcko (GENEVE) for providing their simulation codes. This work was supported in part by the Natural Science and Engineering Research Council of Canada (NSERC) and by the Fonds pour la Formation de Chercheurs et l'Aide à la Recherche (FCAR, Québec).

REFERENCES

1. L.G. Moretto and G.J. Wozniak, Ann. Rev. Nucl. Sci **43**, 379 (1993) and refs. therein.
2. W. A. Friedman, Phys. Rev. Lett. **60**, 2125, (1988).
3. W. A. Friedman, Phys. Rev. C **42**, 667, (1990).

4. G. Peilert et al., Rep. Prog. Phys. **57**, 553 (1994) and refs. therein.
5. C.P. Montoya et al., Phys. Rev. Lett.**73**, 3070, (1994).
6. J. Tõke et al., Phys. Rev. Lett. **75**, 2920, (1995).
7. J.F. Lecolley et al., Phys. Lett. **B354**, 202, (1995).
8. B. Lott et al., Phys. Rev. Lett. **68**, 3141, (1992).
9. B.M. Quednau et al., Phys. Lett. **B309**, 10, (1993).
10. J.F. Lecolley et al., Phys. Lett. **B325**, 317, (1994).
11. Y. Larochelle et al., Phys. Lett. **B352**, 8, (1995).
12. J. Péter et al., Nucl. Phys. **A593**, 95, (1995).
13. L. Beaulieu et al., Submitted to Phys. Rev. Lett. , (1996).
14. S.B. Gazes et al., Phys. Rev. C **38**, 712 (1988).
15. C. Pruneau et al., Nucl. Phys. **A500**, 168, (1989).
16. J. Pouliot et al., Phys. Lett. **B223**, 16, (1989).
17. K.A. Griffionen et al., Phys. Rev. C **40**, 1647, (1989).
18. R. Wada et al., Phys. Rev. C **39**, 497, (1989).
19. J. Pouliot et al., Phys. Rev. C **43**, 735, (1991).
20. D. Doré et al., Nucl. Phys. **A545**, 363, (1992).
21. C. Schwartz et al., Z. Phys. A **345**, 29, (1993).
22. A. Lleres et al., Phys. Rev. C **48**, 2753, (1993).
23. P. Désesquelles et al., Phys. Rev. C **48**, 1828, (1993).
24. A. Badalà et al., Phys. Rev. C **48**, 633, (1993).
25. R. Laforest et al., Nucl. Phys. **A568**, 350, (1994).
26. L. Beaulieu et al., Nucl. Phys. **A580**, 81, (1994).
27. R.J. Charity et al., Phys. Lett. **B323**, 113, (1994).
28. R.J. Charity et al., Phys. Rev. **52**, 3126, (1995).
29. M. Samri et al., Nucl. Phys. **A583**, 427, (1995).
30. L. Beaulieu et al., Phys. Rev. **C51**, 3492, (1995).
31. M. Samri et al., Accepted for publication in Phys. Lett. B, (1996).
32. W. Trautmann et al., Proceedings of the XXXIII International Winter Meeting on Nuclear Physics, Bormio (Italy), 1995 23-27 January. Ed. I. Iori, Physics Dept, Univ. Milano, p.372, (1995).
33. J. Hubele et al., Phys. Rev. C**46**, 1577, (1992).
34. A. Lleres et al., Phys. Rev. C **50**, 1973, (1994).
35. P. Kreutz et al., Nucl. Phys. A**556**, 672, (1993).
36. C. Pruneau et al., Nucl. Inst. and Meth. **A297**, 404, (1990).
37. Y. Larochelle et al., Nucl. Instr. and Meth. in Phys. Res. **A348**, 167, (1994).
38. J.P. Wielezcko et al., Proceedings of the 2^{nd} TAPS Workshop, Guardamar, Espagne ed. by Diaz, Martinez and Schutz, World Scientific, p.145, (1993).
39. R.J. Charity et al., Nucl. Phys. **A483**, 371, (1988).
40. D. Horn et al., Proceedings of the Workshop on Heavy-Ion Fusion, Padua, Italie, 1994 ed. A.M. Stefanini, G. Nebbia, S. Lunardi, G.Montagnoli and A. Vitturi, World Scientific, p.555, (1994).
41. D. Durand, Nucl. Phys. A **541**, 266, (1992).
42. J. Pan et al., Phys. Lett. B**344**, 29, (1995).
43. J. Pan et al., Phys. Rev. C**51**, 1384, (1995).
44. T. Li et al., Phys. Rev. Lett.**70**, 1924, (1993).
45. S.C. Jeong et al., LPCC 95-12, submitted to Nucl Phys. A, (1996).
46. J.C. Steckmeyer et al., Proceedings of the XXXIII International Winter Meeting on Nuclear Physics, Bormio (Italie), 1995 23-27 Janvier. Ed. I. Iori, Dept Physics, Univ. Milano, p.183, (1995).
47. L. Beaulieu et al., To be submitted, (1996).
48. P. Désesquelles et al., Proceedings of the XXXIII International Winter Meeting on Nuclear Physics, Bormio (Italie), 1995 23-27 Janvier. Ed. I. Iori, Dept Physics, Univ. Milano, p.173, (1995).
49. J.A. Hauger et al., submitted to Phys. Rev. Lett. and Ph. D. Thesis, Purdue Univ., W. Lafayette, IN, unpublished, (1996).
50. M.L. Tincknell et al., Proceeding of the 12th Workshop on Nuclear Dynamics, Snowbird, Utah (USA), 1996 3-10 February. Ed. W. Bauer and G. Westfall, Plenum Press. To be published., (1996).